

Looking into Dark Energy Effect on the Extragalactic Radio Quasar Luminosity Evolution

Abstract: In this work, we use both analytical methods and statistical methods to find effect of dark energy on the extragalactic radio (EGR) quasar luminosity evolution. We carry out linear regression analysis of observed source linear sizes (D) of the more extended radio quasars against their corresponding observed redshifts (z) in our sample. Also, we carry out similar analysis on the observed linear sizes of compact steep spectrum (CSS) quasars against their corresponding observed redshifts. Results of the regressions indicate that if we take D to be distance between any two positions in the environment in which the source is domiciled, then cosmic evolution relates inversely with the distance between the two positions in question – it is given by $(1+z) \sim D^{-\psi}$; where $\psi = 0.6$ and 0.4 for the more extended EGR quasars and CSS quasars respectively. Since “a higher redshift implies an earlier epoch”, and redshift has a direct dependence on expansion velocity between any two points in space, the results of the analyses simply suggest that at earlier epoch, the expansion rate of the universe was higher. Our results also indicate that the effect of cosmic evolution in the extended EGR quasars is more than the effect in the CSS quasars (i.e. $D_{z(EGRQ)} > D_{z(CSSQ)}$). Since the linear sizes of the more extended EGR quasars are projected into the intergalactic medium (IGM), while the linear sizes of the CSS quasars are domiciled within their individual host galaxies (i.e. the interstellar medium [ISM]), the result ($D_{z(EGRQ)} > D_{z(CSSQ)}$) can be interpreted to mean that cosmic evolution shows greater effect in the IGM (i.e. more rarefied medium) than in the ISM (i.e. less rarefied medium). Hence, from the results of the analyses, we may state that if dark energy is defined as the intrinsic tendency of vacuum (or free space) to increase in volume, then the inconsistency in $D_{z(EGRQ)}$ and $D_{z(CSSQ)}$ is simply a manifestation of dark energy. Therefore, we may state that dark energy constitutes a driving parameter behind cosmic evolution. Moreover, semi-empirically, we find that as $\mathcal{P}_{CE[z(CSSQ)]} \gg \mathcal{P}_{CE[z(EGRQ)]}$, $P_{CSSQ} \gg P_{EGRQ}$; where $\mathcal{P}_{CE[z(CSSQ)]}$ and $\mathcal{P}_{CE[z(EGRQ)]}$ are powers of the central engines of CSS quasars and the more extended quasars respectively. P_{CSSQ} and P_{EGRQ} are respectively luminosity of CSS quasars and that of the more extended quasars. It states that the power of the central engine of the CSS quasar is much greater than that of the more extended quasar when matched at the same epoch. This is in harmony with luminosities (P_{CSSQ} and P_{EGRQ}) since they are expected to show power-law function with the source central engine. In conclusion, our results suggest that since the components of the more EGR quasars are in the IGM and $D_{z(EGRQ)} > D_{z(CSSQ)}$, dark energy may be responsible for the diminution effect on their luminosities.

Keywords: dark energy; luminosity, central engine, cosmic evolution; linear size; radio sources; quasars; redshifts.

1. Introduction

The building blocks of the Universe are the galaxies. In terms of their luminosities, galaxies can be classified into sub-groups: namely, normal galaxies and active galaxies. Active galaxies are those galaxies that radiate in excess of $10^{36}W$ [1-4]. Unlike the normal galaxy whose radiation comes from the constituent stars, an active galaxy radiates copious amounts of radiation from its three major components: namely, central engine (believed to harbor a super massive blackhole), two-sided jets emanating from the central engine, and two-sided lobes fed by the jets [1-4].

Active galaxies consist of radio-loud sources and radio-quiet sources. The former are commonly referred

to as extragalactic radio sources (EGRS). EGRS emit large amount of radio emission. They show high ratio of radio to optical emission. This ratio is generally defined by the quotient of the two flux densities given by $S_{5\text{ GHz}}/S_{6 \times 10^5 \text{ GHz}} > 10$ [1-7]. They comprise radio galaxies, radio quasars and BL Lacertae objects [4-8]. Observationally, radio radiation from these EGRS generally assumes the morphology of two opposite sided relativistic jets connecting the base of the accretion disk to two radio-emitting lobes straddling the central engine [1-8]. The jet is believed to serve as a conduit through which jets materials reach the lobe. In some sources, the lobes contain hotspots believed to be the termination points of the jets [1-8]. The jets of these sources are projected into the intergalactic medium (IGM). It is good to note that this medium is almost a perfect vacuum where vacuum energy (or dark energy) takes effect.

Compact steep spectrum sources (CSSs), on the other hand, belong to this class of active galaxies known as extragalactic radio sources (EGRS) that radiate more in the radio wavelengths [9–14]. The major difference between the CSSs and the more extended EGRSs is their miniaturized nature but yet powerful in radiation [9–14]. They constitute a remarkable class of radio sources accounting for a substantial fraction of the extragalactic sources selected, especially, at high radio frequencies where the source counts are usually dominated by flat spectrum (spectral index, $\alpha < 0.5$, $S_\nu \propto \nu^{-\alpha}$; where S_ν is flux density). They are not just cores that show steep spectra, rather they are full-fledged radio galaxies and quasars complete with jets and lobes, but on small scale [9–14]. They have been shown to contain special characteristics that make them be considered as a separate class of objects in addition to lobe- and core-dominated Active Galactic Nuclei (AGNs). They are usually found at high redshifts (generally, they tend to have redshift distribution of $z \leq 4$), and are among high luminosity sources [9–14]. The CSS sources are sub-galactic in dimension. This implies that their linear sizes are well below 30 Kpc; and their components are buried in the interstellar media (ISM). The more extended EGRSs have linear sizes, D , given by $D > 30$ Kpc assuming Hubble constant, $H_0 = 75 \text{ kms}^{-1}\text{Mpc}^{-1}$. In all cases, their linear sizes extend into the IGM. Their radio luminosity is in excess of 10^{26}W at 5 GHz; and overall luminosities ($P_{bol} \geq 10^{37}\text{W}$) in common with the CSS [4–14].

Furthermore, it has been well noted that presence of jets in radio sources simply suggests presence of gaseous ambient media [15–18]. A number of hydrodynamic simulations of jet propagations have been performed to examine their physical properties [15–16]. These studies show that jet materials have smaller masses than those of the ambient medium. Besides, Ezeugo and Ubachukwu (2010) [13] obtained a model for evolution of CSS sources (which is a subclass of EGRSs) and used it to estimate their ambient densities. In this work, we use analytical and statistical methods to find effect of dark energy on the extragalactic radio sources (EGRS) evolution

Dark energy is simply the intrinsic tendency of vacuum (or free space) to increase in volume. It brings more spaces into existence. This energy is anti-gravity, and is believed to be the driving force behind the evolution (expansion) of the universe [19].

The extragalactic radio sources used in the analyses are obtained from [15]. They are made up of 170 extended radio-loud quasars with observed linear size, $D > 30\text{Kpc}$. The second sample contains 31 CSS

radio-loud quasars obtained from [12]

2. Cosmic Evolution and IGM

In this section we use the more extended EGR quasars in the analyses. The projected linear sizes of these sources are of extragalactic dimension ($D > 30$ Kpc) – their components (jets and lobes) are located in the IGM. This is because the size of a typical galaxy is ≈ 30 Kpc. Therefore, whatever result obtained in this section has been affected by the most rarefied medium – the IGM. We carry out linear regression analysis of observed source linear sizes, D , of the more extended EGR quasars against their corresponding observed redshifts, z , (Figure 1) in our sample.

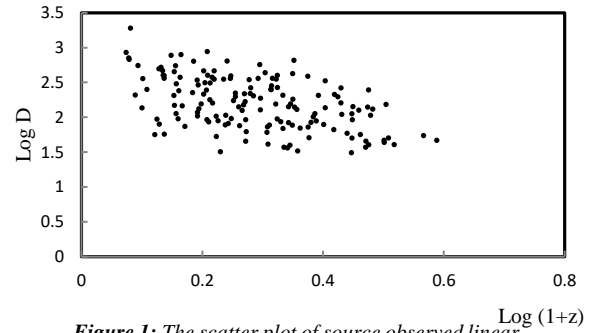


Figure 1: The scatter plot of source observed linear sizes against observed redshifts for extended quasars

Results of the regression show that D relates with z according to the equation:

$$\text{Log} D = -1.595 \text{Log}(1+z) + 2.657 \quad (1)$$

The correlation is good with coefficient, $r = 0.50$; therefore, equation (1) may be rewritten as

$$D \sim (1+z)^{-1.6} \quad (2)$$

Or making $(1+z)$ subject, we obtain

$$(1+z) \sim D^{-0.6} \quad (3)$$

This shows that

$$z = z(D) \quad (4)$$

Therefore, if we take D to be distance between any two positions in the IGM, then equation (3) shows that cosmic evolution has an inverse power-law function with the distance between the two positions. This implies that at earlier epoch, the expansion rate of the universe was higher.

3. Cosmic Evolution and ISM

Here, we use CSS quasars in the analyses. The projected linear sizes of these sources are of sub-galactic dimensions ($D < 30\text{Kpc}$) – their components (jets and lobes) are located in the ISM. Therefore, whatever result obtained in this section has been affected by the dense gases in the interstellar medium.

Ezeugo and Ubachukwu [13] have shown that these radio sources are evolving in dense interstellar media unlike their extended counterparts.

On the $D - z$ plane (Figure 2), we obtain the relation:

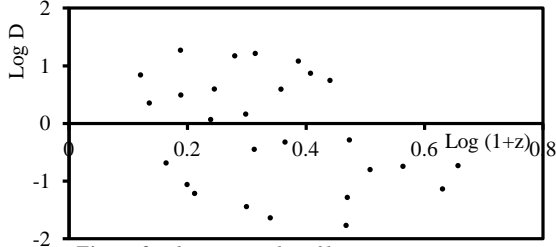


Figure 2: The scatter plot of linear size against redshift for CSS quasars

$$\text{Log} D = -2.49 \text{Log}(1+z) + 0.89 \quad (5)$$

with correlation coefficient, $r = 0.4$. Even though the correlation is marginal, it is still in consonance with the result obtained for the more extended quasars. So, if we assume it is good enough for observed physical parameters such as these, we may transform equation (5) to obtain

$$D \sim (1+z)^{-2.5} \quad (6)$$

Or, as before, we make $(1+z)$ subject, to find

$$(1+z) \sim D^{-0.4} \quad (7)$$

This shows that

$$z = z(D) \quad (8)$$

Therefore, just as pointed out earlier, if we take D to be distance between any two positions in the ISM, then equation (7) shows that cosmic evolution has an inverse power-law function with the distance between the two positions. This also implies that at earlier epoch, the expansion rate of the universe was higher.

4. Dark Energy and Cosmic Evolution

As stated earlier, dark energy is the intrinsic tendency of vacuum (or free space) to increase in volume. It brings more spaces into existence. This energy is anti-gravity, and is believed to be the driving force behind the evolution (expansion) of the universe [19]. From (3) and (7), we have

$$D_{z(\text{EGRQ})} > D_{z(\text{CSSQ})} \quad (9)$$

where $D_{z(\text{EGRQ})}$ represents cosmic evolution effect in the extended quasars, and $D_{z(\text{CSSQ})}$, the effect in CSS quasars. Since the linear sizes of the extended radio-loud quasars jut into the IGM, while the linear sizes of the CSS radio-loud quasars are located within their individual host galaxies, therefore, equation (9) can be interpreted to mean that cosmic evolution shows

greater effect in the IGM (more rarefied medium) than in the ISM (less rarefied medium). Hence, from the foregoing, we may state that if dark energy is defined as the intrinsic tendency of vacuum (or free space) to increase in volume [19], then the inconsistency in $D_{z(\text{EGRQ})}$ and $D_{z(\text{CSSQ})}$ is simply the manifestation of dark energy.

5. Power of the Central Engine

The standard beam model for EGRS in general states that jet materials (presumably electrons) are ejected from the central engine [1,8,12,13]. They plough their way through the ambient medium until they terminate with strong shocks (i.e. hotspots) which are thermalized to form lobes [1,8,12,13]. Therefore, dynamical evolution of a radio source should be expected to depend (in addition to other factors) on the following factors: (i) power of the central engine, (ii) time, and (iii) the density of the ambient medium. Hence, we can write

$$D \sim \mathcal{P}_{\text{CE}}^{\gamma} \mathcal{T}^{\mu} \rho^{\sigma} \quad (10)$$

where D is projected source linear size, \mathcal{P}_{CE} is power of the central engine, ρ is density of ambient medium, \mathcal{T} is time. The indices are not yet known. Assuming a uniform medium, jet velocity, v_j , may be defined as

$$v_j = \frac{dD}{d\mathcal{T}} \quad (11)$$

So that source age may be expressed as

$$\mathcal{T} = \int_{\mathcal{T}_1}^{\mathcal{T}_2} \frac{dD}{v_j} \quad (12)$$

where \mathcal{T}_1 represents the time jet materials started shooting out from the central engine; while \mathcal{T}_2 represents the present epoch. From equations (10) and (12), we obtain

$$D \sim \mathcal{P}_{\text{CE}}^{\gamma} \rho^{\sigma} \left(\int_{\mathcal{T}_1}^{\mathcal{T}_2} \frac{dD}{v_j} \right)^{\mu} \quad (13)$$

For simplicity, we assume ram-pressure balance between the jet and the ambient medium; therefore, we have [8,11,12,13]

$$p_j \approx \rho m_h v_j^2 \quad (14)$$

where p_j is jet internal pressure, m_h is hydrogen mass.

Or for jet velocity, we obtain

$$v_j \approx \sqrt{\frac{p_j}{\rho m_h}} \quad (15)$$

Combining equations (13) and (15), we have

$$D \sim \mathcal{P}_{\text{CE}}^{\gamma} \rho^{\sigma} \left(\int_{\mathcal{T}_1}^{\mathcal{T}_2} \sqrt{\frac{\rho m_h}{p_j}} dD \right)^{\mu} \quad (16)$$

which yields

$$\sqrt{\frac{\rho m_h}{p_j}} \sim \frac{d \left(\frac{D}{\mathcal{P}_{CE}^\gamma \rho^\sigma} \right)^{\frac{1}{\mu}}}{dD} \quad (17)$$

Assuming

$$\frac{d \left(\frac{D}{\mathcal{P}_{CE}^\gamma \rho^\sigma} \right)^{\frac{1}{\mu}}}{dD} \approx (\mathcal{P}_{CE}^\gamma \rho^\sigma)^{-\frac{1}{\mu}} \quad (18)$$

then, (17) becomes

$$\sqrt{\frac{\rho m_h}{p_j}} \sim (\mathcal{P}_{CE}^\gamma \rho^\sigma)^{-\frac{1}{\mu}} \quad (19)$$

Solving for the power of the central engine, we obtain

$$\mathcal{P}_{CE} \sim \rho^{-\frac{\sigma}{\gamma}} \left(\frac{\rho m_h}{p_j} \right)^{\frac{\mu}{2\gamma}} \quad (20)$$

Or in simple terms, we may write

$$\mathcal{P}_{CE} \sim \rho^{-\left(\frac{2\sigma+\mu}{2\gamma}\right)} p_j^{\frac{\mu}{2\gamma}} \quad (21)$$

where hydrogen mass, m_h , is a constant. If we let $\beta \equiv -\left(\frac{2\sigma+\mu}{2\gamma}\right)$ and $\psi \equiv \frac{\mu}{2\gamma}$, the last equation becomes

$$\mathcal{P}_{CE} \sim \rho^\beta p_j^\psi \quad (22)$$

Equation (22) may be interpreted to mean that if every other factor is constant, the radio jet derive its power from the central engine; while the magnitude of the power of the central engine depends on the density of the source ambient medium.

6. Size/Luminosity Relation (Theory)

We can show that source luminosity is attenuated by the particles of the medium as distance from the central engine increases; this is given by

$$P \approx (m_h c^3 \Omega \epsilon)^{-1} \frac{1}{D^2 \rho} \quad (23)$$

where P is source luminosity, c is speed of light, Ω is jet opening solid angle, D is source linear size, ϵ is conversion efficiency of matter into radiation. Combining equations (22) and (23), we obtain

$$\mathcal{P}_{CE} \sim \left(\frac{1}{m_h c^3 \Omega \epsilon D^2 P} \right)^\beta p_j^\psi \quad (24)$$

Equation (24) also shows that the magnitudes of source size and luminosity depend on the power of the central engine. This may be expressed as

$$\mathcal{P}_{CE} \sim (D^2 P)^{-\beta} \quad (25)$$

where the indices in equations (24) and (25) are to be determined.

Let Q be an unknown constant; therefore, equation (24) can be rewritten as

$$\mathcal{P}_{CE} = Q \left(\frac{1}{m_h c^3 \Omega \epsilon D^2 P} \right)^\beta p_j^\psi \quad (26)$$

Furthermore, solving for source projected linear size,

we have

$$D = \left[\frac{1}{m_h c^3 \Omega \epsilon} \left(\frac{Q p_j^\psi}{\mathcal{P}_{CE}} \right)^{\frac{1}{\beta}} \right]^{\frac{1}{2}} P^{-0.5} \quad (27)$$

The last equation simply suggests that the indices, β and ψ , may be estimated from $D - P$ data.

7. Size/Luminosity Relation (Empirical)

From $D - P$ data for larger quasars (Figure 3), we find the relation,

$$\text{Log } D = 66.34 - 38.93 \text{Log } P \quad (28)$$

(with correlation coefficient, $r = 0.52$), which connects the source linear size, D , and luminosity, P . Making D subject, we obtain

$$D = 1.82 P_{EGRQ}^{-39} \quad (29)$$

where $P \equiv P_{EGRQ}$. This shows that observed source size has an inverse power-law function with observed luminosity.

Writing the constant in power of ten, gives

$$D = 10^{0.26} P_{EGRQ}^{-39} \quad (30)$$

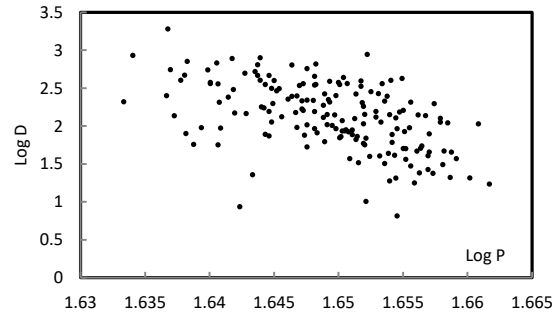


Figure 3: The scatter plot of source observed linear sizes against observed luminosities for extended quasars

Moreover, we carry out linear regression analysis of observed source linear sizes of CSS quasars against their individual observed luminosities (Figure 4).

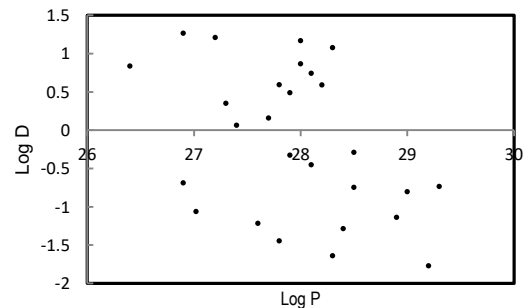


Figure 4: The scatter plot of source observed linear sizes against observed luminosities for CSS Quasars

Result of the regression shows that D relates with P according to the expression:

$$\text{Log}D = -0.57\text{Log}P + 15.88 \quad (31)$$

The correlation is appreciable with coefficient, $r = 0.43$; therefore, we may re-write equation (30) as

$$D = 7.6 \times 10^{15} P_{CSSQ}^{-0.6} \quad (32)$$

where $P \equiv P_{CSSQ}$. Writing the constant in power of ten as before, gives

$$D = 10^{15.88} P_{CSSQ}^{-0.6} \quad (33)$$

When compared with equation (27), equation (33) is in consonance with it; while equation (30) is out of consonance with it. Moreover, comparing the two equations with each other, we find that

$$P_{CSSQ} \gg P_{EGRQ} \quad (34)$$

This shows that there is/are factor(s) that cause(s) diminution effect on the luminosities, P_{EGRQ} , of larger quasars. In absence of any other factors, dark energy appears to be the culprit. This implies that creation of more spaces in the IGM by dark energy dilutes the source luminosities.

For the sake of comparing the constants of equations (30) and (33), we equate the indices of the terms in the brackets of equations (26) to those of equations (30) and (33) individually to obtain $\beta \approx 1.92$ with $\psi = 0.52$ for the extended quasars, and $\beta \approx 0.03$ with $\psi = 32$ for CSS quasars. Putting the values of the indices into equation (27), we obtain for extended quasars (in one significant figure),

$$\mathcal{P}_{CE[z(EGRQ)]} = \mathcal{G} \left(\frac{1}{m_h c^3 \Omega_E D^2 P} \right)^2 p_j^{0.52} \quad (35)$$

while similarly for CSS quasars, we have

$$\mathcal{P}_{CE[z(CSSQ)]} = \mathcal{H} \left(\frac{1}{m_h c^3 \Omega_E D^2 P} \right)^{0.03} p_j^{32} \quad (36)$$

\mathcal{G} and \mathcal{H} are new constants that take care of **the old one (Q)** and new constants during the last mathematical operation. The last two relations may be interpreted to mean that in absence of external factors, the source central engine fuels the observed physical **properties** of these radio quasars.

Combining equations (2) & (35); and equations (6) & (36) yield respectively, we get

$$\mathcal{P}_{CE[z(EGRQ)]} = \mathcal{G} \left(\frac{(1+z)^{3.2}}{m_h c^3 \Omega_E P} \right)^2 p_j^{0.52} \quad (37)$$

and

$$\mathcal{P}_{CE[z(CSSQ)]} = \mathcal{H} \left(\frac{(1+z)^5}{m_h c^3 \Omega_E P} \right)^{0.031} p_j^{32} \quad (38)$$

Hence, for simplicity we obtain respectively,

$$(1+z) \sim \mathcal{P}_{CE[z(EGRQ)]}^{0.16} \quad (39)$$

and

$$(1+z) \sim \mathcal{P}_{CE[z(CSSQ)]}^{6.45} \quad (40)$$

which implies that

$$\mathcal{P}_{CE[z(CSSQ)]} \gg \mathcal{P}_{CE[z(EGRQ)]} \quad (41)$$

The last expression states that the power of the central engine of the CSS quasar is much greater than that of the more extended quasar when matched at the same epoch. This is in support of equation (34) since source luminosity is expected to depend on the power of the source central engine.

8. Discussion and Conclusion

We have carried out linear regression analysis of observed source linear sizes (D) of the more extended radio quasars against their corresponding observed redshifts, z , (Figure 1) in our sample. Results of the regression analysis show that D relates with z according to equation (3), $(1+z) \sim D^{-0.6}$, with correlation coefficient, 0.50. The correlation is good. Therefore, if we take D to be distance between any two positions in the IGM, then the relation shows that cosmic evolution has an inverse power-law function with the distance between the two positions. Since “a higher redshift implies an earlier epoch”, and redshift has a direct dependence on expansion velocity between any two positions (according to Hubble’s law), then the results of the analyses simply suggest that at earlier epoch, the expansion rate of the universe was higher.

Moreover, on the $D - z$ plane (Figure 2), we obtain the relation, $(1+z) \sim D^{-0.4}$ (i.e. equation [7]), which connects the observed linear sizes of CSS quasars and their respective redshifts. The correlation is marginal with, $r = 0.4$. However, we take it to be appreciable enough for observable data. Therefore, just as pointed out earlier, if we take D to be distance between any two positions in the ISM, then equation (7) shows that cosmic evolution has an inverse power-law function with the distance between the two positions. This also shows that since “observation of a higher redshift implies observation at an earlier epoch” (and as pointed out earlier – according to Hubble’s law, redshift has a direct dependence on expansion velocity between any two points in space), then the results of the analyses simply suggest that at earlier epoch, the expansion rate of the universe was higher.

From equations (3) and (7), we find that the effect of cosmic evolution in the extended quasars is more than the effect in the CSS quasars (i.e. $D_{z(EGRQ)} > D_{z(CSSQ)}$). Since the linear sizes of the extended radio-loud quasars are projected into the IGM, while the linear sizes of the CSS quasars are confined within their individual host galaxies, equation (9) can be

interpreted to mean that cosmic evolution shows greater effect in the IGM (more rarefied medium) than in the ISM (less rarefied medium). Hence, from the results of the analyses, we may state that if dark energy is defined as the intrinsic tendency of vacuum (or free space) to increase in volume, then the inconsistency in $D_{z(EGRQ)}$ and $D_{z(CSSQ)}$ is simply a manifestation of dark energy. Therefore, we may conclusively say that dark energy constitutes a driving parameter behind cosmic evolution. The particle number density of the ISM of CSS quasars has been estimated by Ezeugo and Ubachukwu [13]. Their results show that the estimated ambient (ISM) densities of CSS quasars generally, by far, outweigh those of their extended counterparts.

Moreover, we show that source luminosity is attenuated by the particles of the medium as distance from the central engine increases; this is given by $P \approx (m_h c^3 \Omega \epsilon)^{-1} \frac{1}{D^{2\beta}}$ (see equation [23]). where the symbols have their usual meanings. Combining equations (22) and (23), we obtain equation (24); i.e. $\mathcal{P}_{CE} \sim \left(\frac{1}{m_h c^3 \Omega \epsilon D^{2\beta}} \right)^\beta p_j^\psi$. This equation shows that the magnitudes of source size and luminosity depend on the power of the central engine. The indices, β and ψ , are to be estimated. We let Q be an unknown constant; therefore, (24) may be rewritten as $\mathcal{P}_{CE} = Q \left(\frac{1}{m_h c^3 \Omega \epsilon D^{2\beta}} \right)^\beta p_j^\psi$. Furthermore, we solve for source projected linear size, and get equation (27); i.e.

$$D = \left[\frac{1}{m_h c^3 \Omega \epsilon} \left(\frac{Q p_j^\psi}{\mathcal{P}_{CE}} \right)^{\frac{1}{\beta}} \right]^{\frac{1}{2}} P^{-0.5}. \quad (27)$$

This equation simply shows that β and ψ may be estimated from linear regression of the D/P data.

From $D - P$ data for the more extended quasars (Figure 5), we find the relation, $D = 1.82 P_{EGRQ}^{-0.39}$ (i.e. equation [29]), with correlation coefficient, $r = 0.52$, which connects the source linear size, D , and luminosity, P ; where $P \equiv P_{EGRQ}$. This shows that observed source size has an inverse power-law function with observed luminosity. Writing the constant in power of ten, we obtain equation (30); i.e. $D = 10^{0.26} P_{EGRQ}^{-0.39}$.

Also, we carry out similar analysis on observed source linear sizes against their individual observed luminosities of CSS quasars (see Figure 4). Result of the regression shows that D relates with P according to the expression, $D = 10^{15.88} P_{CSSQ}^{-0.6}$ (equation [33]). The correlation is appreciable with coefficient, $r = 0.43$. When compared to equation (27), equation (33) is in consonance with it; while equation (30) is out of

consonance with it. Moreover, comparing equations (30) and (33), we find that $P_{CSSQ} \gg P_{EGRQ}$. This shows that there is/are factor(s) that cause(s) attenuation of luminosities, P_{EGRQ} , of larger quasars. In absence of any other factors, dark energy appears to be a suspect since we have found earlier that $D_{z(EGRQ)} > D_{z(CSSQ)}$. This implies that creation of more spaces in the IGM by dark energy dilutes the source luminosities.

For the sake of comparing the constants of equations (30) and (33), we equate the indices of the terms in the brackets of equations (26) to those of equations (30) and (33) individually to obtain $\beta \approx 1.92$ with $\psi = 0.52$ for the extended quasars, and $\beta \approx 0.03$ with $\psi = 32$ for CSS quasars. Putting the values of the indices into equation (27), we obtain for extended quasars (in one significant figure), equations (35) and (36); i.e. $\mathcal{P}_{CE[z(EGRQ)]} = \mathcal{G} \left(\frac{1}{m_h c^3 \Omega \epsilon D^{2\beta}} \right)^2 p_j^{0.52}$ and

$$\mathcal{P}_{CE[z(EGRQ)]} = \mathcal{H} \left(\frac{1}{m_h c^3 \Omega \epsilon D^{2\beta}} \right)^{0.03} p_j^{32} \quad \text{respectively.}$$

where \mathcal{G} and \mathcal{H} are new constants which ensure accuracy during the preceding algebraic operation. Equations (35) and (36) may be interpreted to mean that in absence of external factors, the source central engine fuels the observed physical properties of these radio sources.

Combining equations (2) & (35), and equations (6) & (36) yield respectively, equations (39) and (40); i.e. $(1+z) \sim \mathcal{P}_{CE[z(EGRQ)]}^{0.16}$ and $(1+z) \sim \mathcal{P}_{CE[z(CSSQ)]}^{6.45}$. Hence, we find $\mathcal{P}_{CE[z(CSSQ)]} \gg \mathcal{P}_{CE[z(EGRQ)]}$; i.e. equation (41). It states that the power of the central engine of the CSS quasar is much greater than that of the more extended quasar when matched at the same epoch. This is in harmony with equation (34) since source luminosity is expected to depend on the power of the source central engine. Conclusively, our results suggest that since the components (jets and lobes) of the more extended EGR quasars are in the IGM and $D_{z(EGRQ)} > D_{z(CSSQ)}$, dark energy may be responsible for the diminution effect on their luminosities.

References

- [1]. Robson, I. (1996) Active Galactic Nuclei, John Wiley and Sons Ltd, England.
- [2]. Urry, C.M. (2004) AGN Unification: An Update. Astronomical Society of the Pacific conference series 1. No vol.
- [3]. Ezeugo, J.C. (2021) On Cosmic Epoch and Linear Size/Luminosity Evolution of Compact Steep

- Spectrum Sources. *American Journal of Astronomy and Astrophysics*. 9(1): 8–12.
- [4]. Ezeugo, J.C. (2021) Jet in the More Extended Radio Sources and Unification with Compact Steep Spectrum Sources. *The Pacific Journal of Science and Technology*. 22: 14 – 19.
 - [5]. Ubah, O.L., Ezeugo, J.C.(2021) Relativistic Jet Propagation: Its Evolution and Linear Size Cosmic Dilation. *International Astronomy and Astrophysics Research Journal*. 3(3): 1–6.
 - [6]. Ezeugo, J.C. (2021) On the Intergalactic Media Densities, Dynamical Ages of Some Powerful Radio Sources and Implications. *Journal of Physical Sciences and Application*. 11 (1): 29–34.
 - [7]. Jackson, J.C. (1999) Radio Source Evolution and Unified Schemes. *Publications of Astronomical Society of the Pacific*. 16: 124–129.
 - [8]. Readhead, A.C. (1995) Evolution of Powerful Extragalactic Radio Sources. In *proc. Colloquium on Quasars and Active Galactic Nuclei*, ed. Kohen, M., and Kellermann, K. (USA: National Academy of Sciences, Berkman Center, Irvine), 92, 11447–11450.
 - [9]. Ezeugo, J.C. (2015) Compact Steep-Spectrum Radio Sources and Ambient Medium Density. *International Journal of Astrophysics and Space Science*. 3(1): 1–6.
 - [10]. Ezeugo J.C. (2015) On the Dependence of Spectral Turnover on Linear Size of Compact Steep-Spectrum Radio Sources. *International Journal of Astrophysics and Space Science*. 3(2): 20–24.
 - [11]. Fanti, C., Fanti, R. Dallacasa, D. Schilizzi, R.T. Spencer, R.E. and Stanghellini, C. (1995) Are compact steep spectrum sources young? *Astronomy and Astrophysics*. 302: 317–326.
 - [12]. O’Dea, C.P. (1998) The Compact Steep Spectrum and Gigahertz peaked spectrum radio sources. *Publications of the Astronomical Society of the Pacific*. 110: 493–532.
 - [13]. Ezeugo, J.C. and Ubachukwu, A.A. (2010) The Spectral Turnover–Linear Size Relation and the Dynamical Evolution of Compact Steep Spectrum Sources. *Monthly Notices of the Royal Astronomical Society*. 408: 2256–2260.
 - [14]. Ezeugo J.C. (2021) Compact Steep Spectrum Source Size and Cosmological Implication. *Journal of Research in Applied Mathematics*. 7(2): 1–4.
 - [15]. Nilsson, K. (1998). Kinematical Models of Double Radio Sources and Unified Scheme. *Monthly Notices of the Royal Astronomical Society*. 132: 31–37.
 - [16]. Kawakatu, N. and Kino, M. (2007) The Velocity of Large-scale Jets in a Declining Density Medium. In *Serie de Conferencias. Triggering Relativistic Jets*, ed. W.H. Lee and E. Ramirez-Ruiz. 27: 192–197.
 - [17]. Mahatma, V.H., Hardcastle and, M.J. Williams, W.L.(2019). LoTSS DR1: Double-double Radio Galaxies in the HETDEX Field. *Astronomy and Astrophysics*. 622:A13.
 - [18]. Mingo, B., Croston, J.H. and Hardcastle, M. J. (2019). Revisiting the Fanaroff-Riley Dichotomy and Radio Galaxy Morphology with the LOFAR Two-Meter Sky Survey (LoTSS). *Monthly Notices of the Royal Astronomical Society*. 488:2701–2721.
 - [19]. Friedman, J.A., Turner, M.S. Huterer, D. (2008) Dark Energy and the Accelerating Universe. *Annual Review of Astronomy*. 46: 385–432.